Catalysis Science & Technology

PAPER

View Article Online
View Journal | View Issue

Cite this: *Catal. Sci. Technol.*, 2019, 9, 842

Interplay of nucleophilic catalysis with proton transfer in the nitrile reductase QueF from *Escherichia coli*†

Jihye Jung,[ab] Jan Braun,[a] Tibor Czabany[ab] and Bernd Nidetzky *[ab]

Enzymatic transformations of the nitrile group are important in biology as well as in synthetic chemistry. The enzyme QueF catalyses the conversion of 7-cyano-7-deazaguanine ($preQ_0$) to 7-aminomethyl-7-deazaguanine ($preQ_1$), a unique approach towards biological four-electron reduction of a nitrile to an amine. The catalytic reaction involves a QueF–$preQ_0$ thioimidate adduct that is converted to $preQ_1$ in two NADPH dependent reduction steps *via* an imine intermediate. The QueF active site comprises a cysteine nucleophile flanked by an aspartic acid and additionally contains a histidine. Here, we used mutagenesis of *E. coli* QueF (C190A, C190S, D197A, D197H, and H229A) to study the functional interplay between these enzyme residues in covalent catalysis. Substitution of Cys190 or Asp197 annihilates $preQ_0$ covalent binding and largely disrupts the nitrile-to-amine reductase activity. The H229A variant readily forms the thioimidate adduct and is 24-fold less active for $preQ_0$ reduction than wild-type ecQueF (k_{cat} = 7.2 min^{-1}). Using isothermal titration calorimetry, we show that the non-covalent step of $preQ_0$ binding involves proton uptake mediated by Asp197 with His229 as the likely protonated group. Catalytic proton transfer from the Cys190 thiol *via* Asp197 to the nitrile nitrogen promotes the covalent intermediate. We suggest that protonated (charged) His229 facilitates the polarization of the substrate nitrile for nucleophilic attack on carbon by Cys190, and through proton relay *via* Asp197, it could provide the proton for re-protonating Cys190 during the formation of the imine intermediate.

Received 12th November 2018,
Accepted 11th January 2019

DOI: 10.1039/c8cy02331j

rsc.li/catalysis

Introduction

Enzymatic transformations of the nitrile group are important biologically, for example, in secondary and xenobiotic metabolisms of plants and microorganisms.[1–3] They also have significant applications in synthetic chemistry wherein nitriles often represent important intermediates.[4,5] The nitrile group is converted by hydrolytic enzymes to an amide or to a carboxylic acid[6–9] and by reductive enzymes to an amine.[10–13] Despite the different reactivities, nitrile-converting enzymes share covalent catalysis from an active-site nucleophile as a common feature of their mechanisms. Nitrilase[8,9,14–16] and nitrile reductase[17–20] both utilize a cysteine to form a thioimidate adduct between the enzyme and nitrile substrate (Scheme 1A). The covalent catalysis in each enzyme requires assistance from catalytic proton transfer. The enzyme nucleophile is activated by deprotonation. Conversion of nitrile to the covalent intermediate and further on to the product necessitates acid–base catalysis, as shown in Scheme 1A. Nitrile reductase and nitrilase both have a candidate acid–base residue (Asp or Glu) positioned close to their cysteine nucleophile[8,9,11,16,18,21] but the precise role of the Asp/Glu remains to be elucidated. Moreover, the critical interplay between nucleophilic and general acid–base catalysis is not well understood in both enzymes. In this study, therefore, we sought to clarify the involvement of catalytic proton transfer in the build-up and degradation of the covalent thioimidate intermediate during enzymatic nitrile reduction.

The biological principle of nitrile reduction is embodied in the enzyme QueF.[12,22–26] The natural reaction of QueF is conversion of 7-cyano-7-deazaguanine ($preQ_0$) to 7-aminomethyl-7-deazaguanine ($preQ_1$) by NADPH (Scheme 1B).[17–19,21,27,28] QueF is a bacterial enzyme from the biosynthetic pathway for the modified nucleoside queuosine (Q).[12,22,29] Inserted into tRNA as $preQ_1$ and further converted to Q, queuosine modulates the codon–anticodon binding efficiency for decoding NAC/U codons to Asn, Asp, His, and Tyr.[22,29,30] The proposed catalytic mechanism of QueF is summarized in Scheme 1B. The core characteristics of this mechanism are well supported by enzyme crystal structures and biochemical evidence.[17,18,21,27,28] Therefore, the

[a] *Institute of Biotechnology and Biochemical Engineering, Graz University of Technology, NAWI Graz, Petersgasse 12/1, A-8010 Graz, Austria. E-mail: bernd.nidetzky@tugraz.at*
[b] *Austrian Centre of Industrial Biotechnology, Petersgasse 14, A-8010 Graz, Austria*

† Electronic supplementary information (ESI) available: Raw data of protein mass analysis. See DOI: 10.1039/c8cy02331j

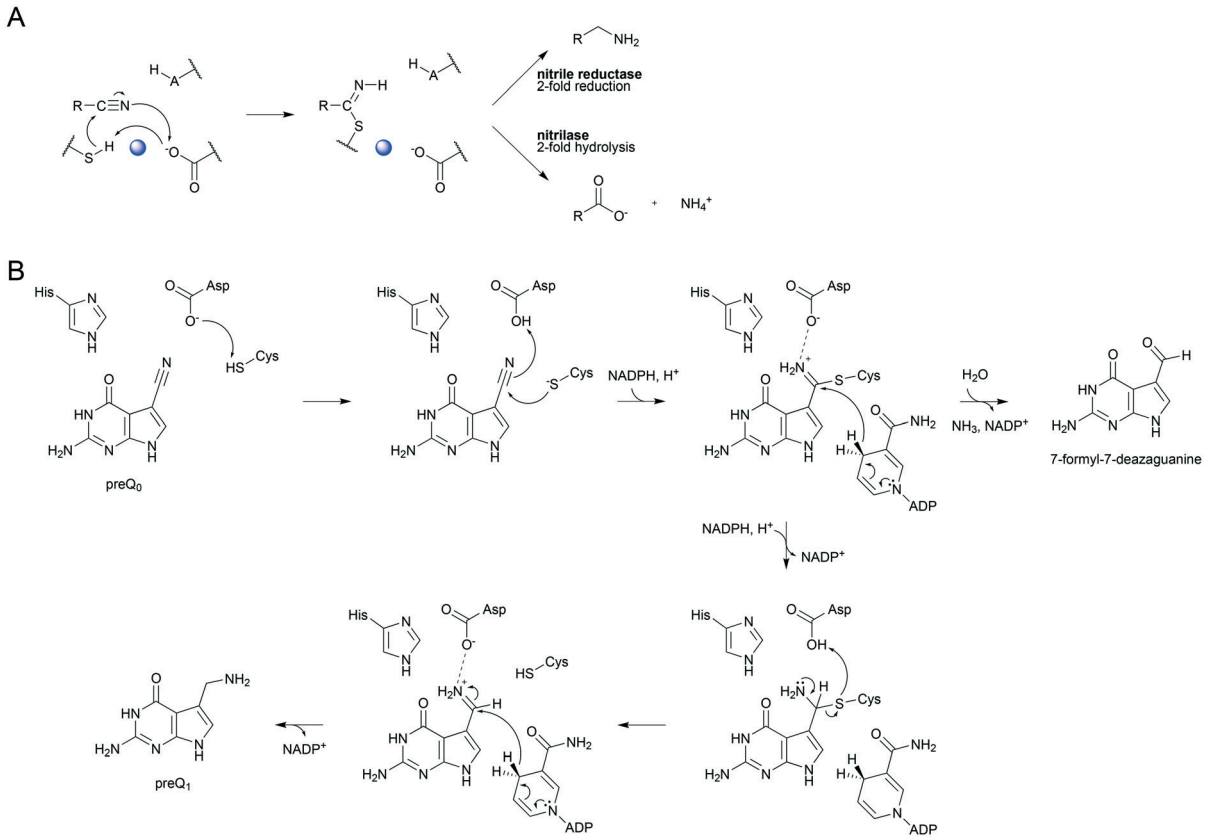

Scheme 1 Mechanistic analogies of nitrile reductase and nitrilase (A) and the proposed mechanism of nitrile reduction by ecQueF (B). (A) Catalytic conversion of the nitrile substrate *via* a common covalent thioimidate enzyme intermediate is shown. Base-catalyzed activation of the cysteine nucleophile is water-mediated in the nitrilase. The water is shown in blue. Reduction and hydrolysis of the thioimidate both involve general acid–base catalysis. (B) A detailed mechanism of $preQ_0$ reduction is shown. Interception of the imine intermediate by water results in the formation of 7-formyl-7-deazaguanine. This off-reaction is not significant in wildtype ecQueF but occurs in certain variants of the enzyme.[27]

thioimidate adduct is formed from a non-covalent QueF–$preQ_0$ complex that secludes the nitrile substrate completely from the solvent (Schemes 1B and 2).[17–20] The covalent intermediate is converted to $preQ_1$ in two NADPH dependent reduction steps *via* an imine. The imine is sequestered effectively in the QueF active site to prevent its decomposition.[17,27] NADPH binds very tightly to the enzyme–imine complex.[17] The enzyme thus ensures that every $preQ_0$ converted is reduced fully to $preQ_1$.

QueF structures reveal that the cysteine catalytic nucleophile is flanked by an aspartic acid. These two residues form the immediate catalytic center (Fig. 1A and B).[18,21,31] A histidine residue is additionally present. In the enzyme from *E. coli* studied here (ecQueF), the relevant residues are Cys190, Asp197 and His229 and this amino acid numbering is used throughout.[11,12,17,27] QM/MM computational analysis of the reaction path of QueF (from *Vibrio cholerae*, vcQueF) suggested involvement of Asp197 in each catalytic step (Scheme 1B).[28] In thioimidate formation, Asp197 would deprotonate Cys190 to subsequently protonate the nitrile nitrogen atom of the $preQ_0$ substrate. In the first and second steps of reduction by NADPH, respectively, Asp197 would stabilize positive charge development on the reactive nitrogen of the protonated thioimidate and imine intermediate. Additionally, upon decomposition of covalent thiohemiaminal to non-covalently bound imine, Asp197 would re-protonate Cys190. In the proposed mechanism,[28] His229 had no immediate role and was excluded from involvement in proton transfer. However, the computational study started from the non-covalent complex between the enzyme and $preQ_0$, not from the free enzyme, and it did not include macromolecular dynamics in the calculations. It also did not evaluate whether variation in the protonation states of the active-site residues affects the catalytic reaction. Crystal structures of thioimidate enzyme–$preQ_0$ adducts of vcQueF and QueF from *Bacillus subtilis* (bsQueF) both reveal a hydrogen bond network connecting the thioimidate N10 *via* Asp197 Oδ2 and an intermediary water to His229 Nδ1, as shown in

$$\text{QueF} + \text{preQ}_0 \rightleftarrows \text{QueF}{\bullet}\text{preQ}_0 \rightleftarrows \text{QueF-preQ}_0$$

Scheme 2 Two-step mechanism of $preQ_0$ binding to QueF. QueF·$preQ_0$, noncovalent complex; QueF–$preQ_0$, covalent thioimidate adduct. In wildtype ecQueF, the conversion of QueF·$preQ_0$ to QueF–$preQ_0$ is irreversible within limits of detection.[17]

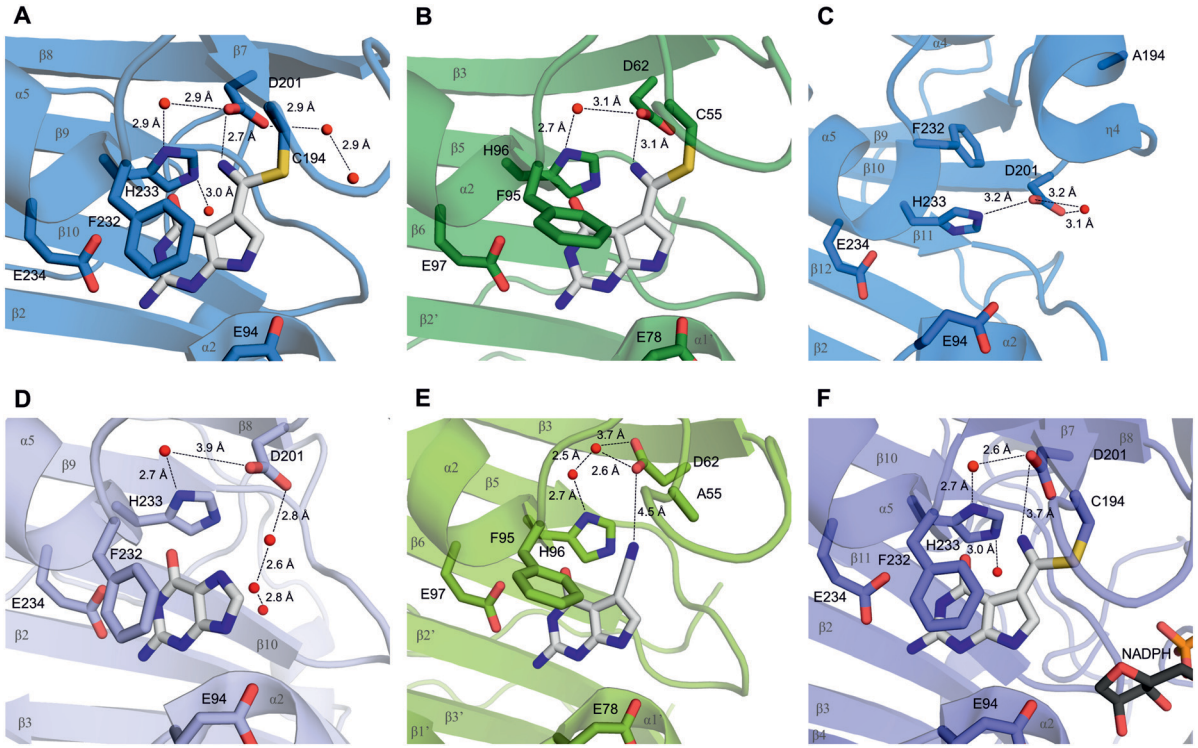

Fig. 1 Crystallographic evidence for a possible proton relay involving the conserved Asp and His residues in QueF active sites. (A and B) The covalent thioimidate adducts between $preQ_0$ and the enzymes are shown for vcQueF (A, R262L variant, PDB code: 3S19) and bsQueF (B, wildtype, PDB code: 4F8B). Water molecules are shown as red balls. The full proton relay involving the substrate, Asp, water and His is established. (C) The apo-enzyme of vcQueF (C194A variant, PDB code: 3RJ4) is shown. (D and E) Noncovalent complexes of vcQueF with guanine (D, C194A variant, PDB code: 3BP1) and bsQueF with $preQ_0$ (E, C55A variant, PDB code: 4FGC) are shown. In panel E, a proton relay involving Asp, water and His is suggested. (F) The covalent $preQ_0$–vcQueF complex with NADPH (R262L variant, PDB code: 3UXJ) is shown. The full proton relay may be functional. In panels A–F, active-site residues are indicated and numbered. Note: the ecQueF residues corresponding to the vcQueF residues are Glu89, Cys190, Asp197, Phe228, His229, and Glu230. Elements of the secondary structure are indicated. In bsQueF (panels B and E) the prime is used to indicate secondary structure elements from another protein subunit. Crystal structures of vcQueF and bsQueF are from ref. 18 and 21 and from unpublished data in the database.

Fig. 1A and B.[18,21] This suggests the possibility of a proton relay involving His229. We have shown in preliminary experiments that $preQ_0$ binding by ecQueF was accompanied by net proton uptake from solution.[17] This finding carries immediate implications for the enzymatic mechanism, but is unaccounted for in the computational reaction path of QueF. In this study, therefore, we used mutagenesis of active-site residues in ecQueF (C190A, C190S, D197A, D197H, and H229A) to study their functional interplay in covalent catalysis for nitrile reduction. We present evidence from kinetic and ligand binding studies that suggests a refined QueF mechanism. In particular, we show that the non-covalent step of $preQ_0$ binding involves proton uptake from His229 *via* Asp197. Catalytic proton transfer from the Cys190 thiol *via* Asp197 to the nitrile nitrogen drives the formation of the covalent intermediate. We also show that His229 has an auxiliary role in ecQueF catalysis. The positive charge on His229 could facilitate the polarization of the substrate nitrile for nucleophilic attack on carbon by Cys190. Through proton relay *via* Asp197, His229 could provide the proton for re-protonation of the cysteine during the formation of the imine intermediate.

Experimental

Chemicals

NADPH (purity >98%) and $NADP^+$ (purity >97%) were from Carl Roth (Karlsruhe, Germany). Materials were of the highest purity available from Carl Roth and Sigma-Aldrich (St. Louis, MO, USA). $preQ_0$ and 7-formyl-7-deazaguanine were synthesized as described previously.[10,17]

Site-directed mutagenesis

Mutagenesis leading to site-directed substitution of Cys190 by Ser (C190S) and Asp197 by Ala (D197A) or His (D197H) was performed according to a standard two-stage PCR protocol.[27,32] A pEHISTEV vector including the ecQueF gene (pEHISTEV:EcNRedWT) was used as the template. The oligonucleotide primers are shown with the mismatched bases underlined.

C190S forward
5′-CTGCTGAAATCAAACAGCCTGATCACCCATCAACC-3′
C190S reverse
5′-GGTTGATGGGTGATCAGGCTGTTTGATTTCAGC-3′
D197A forward

5′-CCTGATCACCCATCAACCAGCGTGGGGTTCGCTCC-3′
D197A reverse
5′-GGAGCGAACCCCACGCTGGTTGATGGGTGATCAGG-3′
D197H forward
5′-CCTGATCACCCATCAACCACATTGGGGTTCGCTCC-3′
D197H reverse
5′-GGAGCGAACCCCAATGTGGTTGATGGGTGATCAGG-3′

Mutagenesis to substitute Cys190 by Ala (C190A) and His229 by Ala (H229A) was reported in an earlier study.[11,17] All mutations were verified by gene sequencing.

Enzyme preparation

The ecQueF variants were obtained as N-terminally His-tagged proteins using expression in *E. coli* BL21-DE3 as described previously.[17,27] All the enzymes were purified by immobilized metal ion affinity chromatography and gel filtration. The enzyme purity (≥99%) was confirmed by SDS-PAGE. The HisTrap affinity column (GE Healthcare, Buckinghamshire, UK) was regenerated fully after each use. The PD10-desalting columns (GE Healthcare) were always freshly used. Contamination with the protein carried over from previous purification runs was thus ruled out rigorously. The protein concentration was measured with a Pierce BCA protein assay kit (Thermo Fisher Scientific, Germering, Germany). Enzyme stock solutions (0.4–0.8 mM) were stored at −20 °C and used up within 3 weeks.

Study of $preQ_0$ binding by ecQueF variants

For isothermal titration calorimetry (ITC), a VP-ITC micro calorimeter from Microcal (Malvern Instruments Ltd., Malvern, UK) was used at 25 °C. The enzyme was gel-filtered twice to phosphate buffer (100 mM Na_2HPO_4–NaH_2PO_4, pH 7.5, additionally containing 50 mM KCl) using illustra NAP 5 columns (GE Healthcare). A DMSO concentration of maximally 2% (v/v) was used in both the enzyme and the $preQ_0$ solution. Experiments were conducted and data evaluation done as described previously.[17,27] The enzyme molar concentration was based on the protein concentration assuming a functional ecQueF homodimer with a molecular mass of 71 740 Da (C190S variant), 71 684 Da (D197A variant), 71 816 Da (D197H variant), or 71 640 Da (H229A variant).

Proton uptake or release in conjunction with ligand binding was determined by ITC experiments done in different buffers featuring different ionization enthalpies (ΔH_{ion}). The principle of the method is that the change in ligand binding enthalpy (ΔH) is determined in dependence of ΔH_{ion}. The slope of the linear relationship between ΔH and ΔH_{ion} indicates the number of protons involved. A positive slope indicates proton uptake; a negative slope means proton release. Besides the phosphate buffer described above, HEPES and Tris buffers (each 100 mM, pH 7.5, additionally containing 50 mM KCl) were used, as reported previously.[17] The number of protons taken up or released was calculated using the equation, $n_{H^+} = (\Delta H_{buffer\ 1} - \Delta H_{buffer\ 2})/(\Delta H_{ion,\ buffer\ 1} - \Delta H_{ion,\ buffer\ 2})$, where n_{H^+} is the number of protons involved in the binding.[33,34] The ΔH_{ion} of phosphate, HEPES, and Tris at pH 7.5 and 25 °C was obtained from the literature as 3.60, 20.40, and 47.45 kJ mol^{-1}, respectively.[35] The values are averages from three independent sets of experiments.

The covalent thioimidate adduct of ecQueF was detected from its characteristic absorbance with maximum absorption at around 380 nm.[17] Absorbance titrations were carried out with a Beckman DU 800 spectrophotometer (Beckman Coulter, Pasadena, CA, USA) as described previously.[17,27] $preQ_0$ was titrated to the enzyme solution in the absence of NADPH.

Quenching of the intrinsic Trp fluorescence is a useful reporter of $preQ_0$ binding, as shown previously for bsQueF and ecQueF.[17,18] Fluorescence titrations were performed using a fluorescence spectrophotometer F-4500 (Hitachi, Ltd., Tokyo, Japan). Emission spectra were recorded in the range 300–500 nm at 1200 nm min^{-1} with an excitation wavelength of 280 nm. $preQ_0$ was titrated to the enzyme solution in the absence of NADPH. The quenching yield was determined as the ratio $(F_0 - F_S)/F_0$, where F_0 and F_S are the protein fluorescence intensities in the absence and presence of the substrate recorded at the same wavelength of emission.

Protein mass analysis

Samples were prepared in Tris-HCl buffer (100 mM, pH 7.5), additionally containing 50 mM KCl and 1.15 mM tris(2-carboxyethyl)phosphine, as described previously.[17] The enzyme and $preQ_0$ concentration was 130 μM and 500 μM, respectively. After the desalting process using Amicon Ultra 0.5 mL centrifugal filters (Merck Millipore, Burlington, MA, USA), a final protein concentration of 30 pmol μL^{-1} was obtained in water containing 5% acetonitrile and 0.1% trifluoroacetic acid. The samples were separated on a capillary HPLC system (Dionex Ultimate 3000, Thermo Fisher Scientific) and analysed in a maXis II electron transfer dissociation mass spectrometer (Bruker, Bremen, Germany) as described in our earlier study of wildtype ecQueF.[17] The captive spray source in positive mode with a mass range of 250–3000 *m*/*z* was used. The obtained protein mass spectra (*e.g.*, D197H variant after incubation with $preQ_0$, see Fig. S1 in the ESI†) were deconvoluted by data analysis software, using the MaxEnt2 algorithm.

Enzymatic reactions of ecQueF variants

$preQ_0$ conversion. Reactions for $preQ_0$ reduction were carried out at 25 °C using agitation at 500 rpm in a Thermomixer Comfort (Eppendorf, Hamburg, Germany). The enzyme concentration was 10 μM (wildtype) or 50 μM (Cys190 and Asp197 variants). The H229A variant was used at 10, 20 and 50 μM. The $preQ_0$ concentration was 250 μM. For the H229A variant, several $preQ_0$ concentrations were used: 50, 100, 150, and 200 μM. The NADPH concentration was 500 μM. Tris-HCl and sodium phosphate buffer (100 mM, pH 7.5), additionally containing 50 mM KCl and 1.15 mM tris(2-carboxyethyl)phosphine, were used. The corresponding

buffers of pH 6.0 and pH 9.0 were also used for the conversion of $preQ_0$ by the D197A variant. Samples were taken at certain times up to 96 h and analysed by HPLC with UV/vis and/or MS detection. All the compounds known to be involved in the reaction according to Scheme 1B ($preQ_0$, $preQ_1$, 7-formyl-7-deazaguanine, NADPH, $NADP^+$) were analysed with the method used.

Absence of nitrile reductase activity in *E. coli* strain background. The cell-free extract of *E. coli* BL21-DE3 harboring the pEHISTEV vector was used. It was prepared using procedures exactly identical to those used for preparing the enzymes. The cell-free extract from BL21-DE3 harboring the pEHISTEV:EcNRedD197A vector for expression of the D197A variant was used as a positive control. The conditions used were as described above, with $preQ_0$ and NADPH concentrations of 250 μM and 500 μM, respectively. The protein concentration in the reaction was 3.6 mg mL^{-1}. For the positive control this would correspond to an estimated concentration of the D197A variant of 50 μM. Samples were analysed by HPLC after 24 h. No $preQ_1$ was formed in the negative control above a detection limit of 1 μM $preQ_1$ formed or 5 μM $preQ_0$ consumed. The positive control showed $preQ_1$ formation (3 μM) as expected.

Proton consumption during $preQ_0$ reduction. This was measured at 25 °C using the pH indicator phenol red using reported protocols.[36,37] Immediately prior to the reaction the wildtype enzyme was gel-filtered twice to a 0.5 mM Tris-HCl buffer (pH 7.51) containing 34 μM phenol red and 150 mM KCl. Reaction mixtures contained 3.6 μM enzyme, 100 μM NADPH and 20–40 μM $preQ_0$. The DMSO concentration was 1% (v/v). Proton consumption was determined by the absorbance increase at 556 nm. The calibration was done with KOH. NADPH conversion was monitored at 340 nm.

HPLC analytics

The products of $preQ_0$ reduction were analysed at 30 °C using an Agilent 1200 HPLC system (Santa Clara, CA, USA) equipped with a 5 μm SeQuant ZIC-HILIC column (200 Å, 250 × 2.1 mm; Merck, Billerica, MA, USA) and the corresponding guard column (20 × 2.1 mm; Merck), and a UV detector (λ = 254, 262 and 340 nm), as described previously.[27]

Results and discussion

Covalent thioimidate formation

The thioimidate adduct of ecQueF with $preQ_0$ is detectable by absorbance with maximum absorption at 380 nm (ε = 10.02 ± 0.14 mM^{-1} cm^{-1}).[17] In assessing ecQueF variants (D197A, D197H, and H229A) for thioimidate formation, the incompetent C190A variant served as a negative control.[11,17] In absorbance titrations wherein $preQ_0$ was used in up to 5-fold molar excess over the enzyme and the wavelength range 300–500 nm was scanned for the absorbance change, no thioimidate adduct was measured for the D197A and D197H variants. The limit of thioimidate detection was ~0.2% of the enzyme concentration used (50 μM). The H229A variant formed the thioimidate adduct similar to the wildtype enzyme. The C190S variant could potentially form a covalent imidate involving serine as the enzyme nucleophile. From absorbance titrations, no evidence for such an intermediate was obtained.

Protein mass analysis confirmed the absorbance data. In wildtype ecQueF, the covalent adduct (35 906.0 ± 1.7 Da) was detected besides the unliganded enzyme (35 732.1 ± 0.5 Da).[17] Only the unliganded enzyme was detected in samples of C190A (35 700 ± 2 Da), C190S (35 716 ± 2 Da) and D197A variants (35 689 ± 2 Da) incubated with $preQ_0$ in 4-fold molar excess over the enzyme subunit present. For the D197H variant, as shown in Fig. 2, mass peaks corresponding to unliganded (35 754 ± 1 Da) and $preQ_0$-bound enzymes (35 929 ± 1 Da) were detected. In the absence of the thioimidate adduct as demonstrated in absorbance titrations, the observable enzyme complex likely involved $preQ_0$ tightly but noncovalently bound.

Noncovalent binding of $preQ_0$

This was analysed with fluorescence titration. Binding of $preQ_0$ is traceable by quenching of protein tryptophan fluorescence.[17,18] We have shown in an earlier study comparing the wildtype and C190A enzyme that fluorescence quenching arises from the noncovalent step of $preQ_0$ binding (Scheme 2).[17] Results for the different ecQueF variants are shown in Fig. 3. The degree of fluorescence quenching at saturating $preQ_0$ was similar in all the enzymes (85–90%). Dissociation constants (K_d) calculated from the data are summarized in Table 1. Among the enzymes not capable of thioimidate formation, the D197H variant showed the highest affinity for $preQ_0$ binding. Its 0.55 μM K_d was on the same order of magnitude as the ~0.1 μM K_d of the H229A variant which binds $preQ_0$ covalently. The D197A variant showed a 25-fold loss of binding affinity as compared to the D197H variant. The K_d of the wildtype enzyme is extremely low (≤3 nM), reflecting nearly irreversible binding of $preQ_0$ as a covalent adduct with the enzyme.[17]

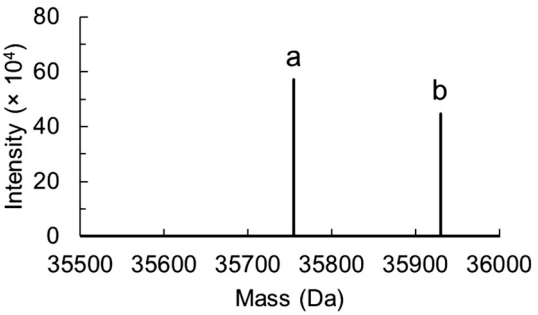

Fig. 2 Protein mass analysis for the D197H variant of ecQueF after incubation with $preQ_0$ is shown. Deconvoluted data was obtained from the protein mass spectrum (see Fig. S1 in the ESI†). The sample is shown to contain both the $preQ_0$-free monomeric protein (a, 35 754 ± 1 Da) and $preQ_0$-bound monomeric protein (b, 35 929 ± 1 Da).

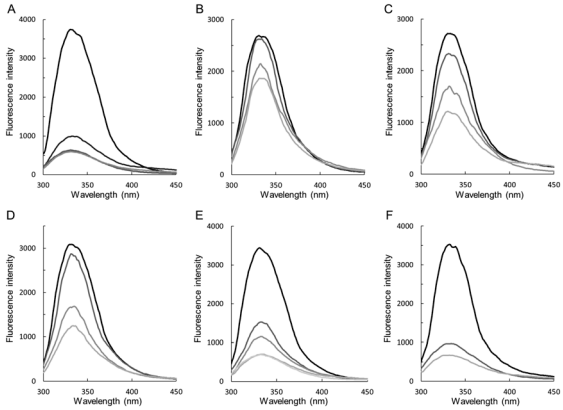

Fig. 3 Fluorescence titration analysis of $preQ_0$ binding to wildtype ecQueF and variants thereof. The enzymes used are wildtype ecQueF (A), C190A (B), C190S (C), D197A (D), D197H (E), and H229A variant (F). The enzyme concentration was 3 μM. Protein fluorescence was quenched upon addition of $preQ_0$ (top to bottom: no $preQ_0$; 1.5, 3, 7.5, 15, and 30 μM $preQ_0$). The K_d values obtained from the data are summarized in Table 1.

Binding of $preQ_0$ analysed with isothermal titration calorimetry

$preQ_0$ binding to ecQueF is a strongly exergonic process that can be monitored well with ITC.[17,27] Of note, a substantial amount (~50%) of the total heat released during $preQ_0$ binding is due to noncovalent complex formation (Scheme 2).[17] ITC data of $preQ_0$ binding to the ecQueF variants in 100 mM phosphate buffer (pH 7.5) are shown in Fig. 4.

The corresponding thermodynamic parameters are summarized in Table 1. For the ecQueF variants unable to form the thioimidate adduct with $preQ_0$, the Gibbs free energy of binding (ΔG) was consistently lower ($\Delta\Delta G$ = +8–12 kJ mol^{-1}) than the corresponding ΔG for the wildtype enzyme. The $\Delta\Delta G$ for the enzyme variants involved a large decrease in the enthalpy of binding ($\Delta\Delta H$ = +36–41 kJ mol^{-1}), thus rendering $preQ_0$ binding less favorable. However, it also involved significant compensation from the entropy term ($-T\Delta S$), which decreased in the variants as compared to the wildtype enzyme. The H229A variant showed a ΔG of binding consistent with that for wildtype ecQueF. However, the ΔH was more negative and the $-T\Delta S$ more positive than in the case of the wildtype enzyme.

The kinetic study of wildtype ecQueF has shown that NADPH binds to both the covalent and the noncovalent complex of the enzyme with $preQ_0$.[17] Binding of NADPH to the $preQ_0$ complex of the C190A variant was previously studied by ITC (Table 1).[17] The 3.6 μM K_d of NADPH binding to this complex was comparable to the corresponding K_d in the wildtype enzyme.[17] Thermodynamic parameters of NADPH binding to the $preQ_0$ complex of the D197H variant were determined (Fig. 4E and Table 1). They are highly similar to the corresponding parameters of the C190A variant. Substitution of Asp197 with a histidine, therefore, does not interfere with binding of NADPH.

Proton uptake during $preQ_0$ reduction

The enzymatic reaction, $preQ_0$ + 2NADPH + 2H$^+$ → $preQ_1$ + 2 NADP$^+$, implies the uptake of two protons for each nitrile substrate converted into the amine product. Assuming a protonated amine in $preQ_1$ at pH 7.5, a third proton would additionally be taken up in the reaction. Time-resolved analysis of proton consumption during $preQ_0$ reduction by wildtype QueF is shown in Fig. 5. The ratio of steady-state rates of proton uptake and NADPH oxidation was 1.5 (± 0.1), consistent with a proton/$preQ_1$ stoichiometry of 3.

Proton uptake during $preQ_0$ binding

The ITC study in buffers (phosphate, Tris, HEPES) differing in ionization enthalpy (ΔH_{ion}) was used to determine proton

Table 1 Thermodynamic parameters of $preQ_0$ binding to wildtype and variant forms of ecQueF

	K_d[a] (μM)		$K_{d\ app}$ (μM)	ΔH_{app} (kJ mol^{-1})	$-T\Delta S_{app}$ (kJ mol^{-1})	ΔG_{app} (kJ mol^{-1})	n_{H^+}	Ref.
Wildtype	≤0.003	Phosphate	0.039	−80.3	37.9	−42.4	0.78 ± 0.09	17
		HEPES	0.034	−65.7	22.9	−42.8		
		Tris	0.054	−47.7	5.1	−41.6		
C190A	46.5	Phosphate	5.5 (3.6)[b]	−44.7 (−31.3)[b]	14.6 (0.07)[b]	−30.1 (−31.2)[b]	0.46 ± 0.27	17
		HEPES	4.26	−42.3	11.5	−30.8		
		Tris	4.05	−23.2	−7.7	−30.9		
C190S	15.3	Phosphate	5.3	−38.9	8.7	−30.2	0.31 ± 0.16	This study
		HEPES	4.6	−36.4	5.8	−30.6		
		Tris	3.7	−23.8	−7.3	−31.1		
D197A	13.7	Phosphate	3.5	−44.3	13.0	−31.3	≈0	This study
		HEPES	3.8	−50	18.9	−31.1		
		Tris	3	−42.7	11	−31.7		
D197H	0.55	Phosphate	1.3 (1.0)[c]	−43.9 (−27.0)[c]	10.1 (−7.5)[c]	−33.8 (−34.4)[c]	0.61 ± 0.05	This study
		HEPES	1.6	−33.1	−0.1	−33.2		
		Tris	1.9	−17.5	−15.3	−32.8		
H229A	≤0.1	Phosphate	0.054	−99.0	57.4	−41.6	1.40 ± 0.37	This study
		HEPES	0.127	−68.9	29.4	−39.5		
		Tris	0.159	−40.2	1.2	−39.0		

[a] Dissociation constants from fluorescence titrations (Fig. 3). [b] NADPH binding to the noncovalent complex of C190A with $preQ_0$. [c] NADPH binding to the noncovalent complex D197H with $preQ_0$.

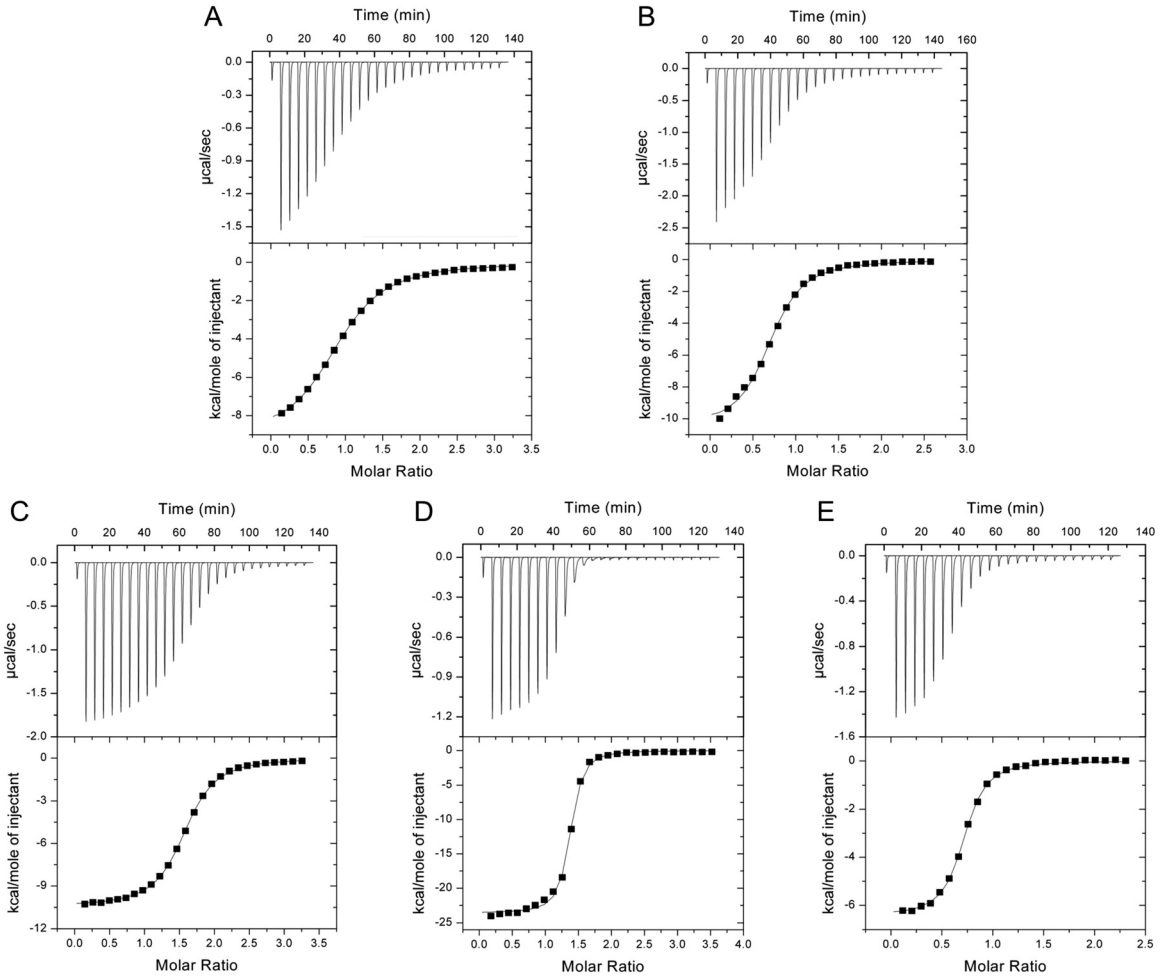

Fig. 4 ITC analysis of $preQ_0$ and NADPH binding to ecQueF variants at 25 °C is shown. Phosphate buffer (100 mM Na_2HPO_4–NaH_2PO_4, pH 7.5) containing 50 mM KCl was used. (A–D) C190S (A, 39 μM), D197A (B, 60 μM), D197H (C, 39 μM), and H229A (D, 8 μM) were used. The $preQ_0$ solution (800 μM for C190S, D197A, and D197H; 250 μM for H229A) was titrated into the enzyme solution. The DMSO concentration did not exceed 2% in both the enzyme and the substrate solution. The *c* values (c = [dimeric protein]/K_d) obtained from the experiments were 7 for C190S, 17 for D197A, 30 for D197H, and 148 for H229A. (E) NADPH (1 mM) was titrated to the noncovalent $preQ_0$–D197H complex (59 μM). The *c* value obtained from the experiment was 59. Results of fits of the data are summarised in Table 1.

uptake/release during $preQ_0$ binding.[17] The change of binding enthalpy ΔH upon variation in ΔH_{ion} is measured and the number of protons exchanged (n_{H^+}) is determined from the slope (positive: proton uptake; negative: proton release) of the linear dependence of ΔH on ΔH_{ion}.[33,34] Results for ecQueF variants are summarized in Table 1 along with previously reported data for the wildtype enzyme and C190A variant. The D197A variant stood out among all other enzymes in that it did not take up protons in conjunction with $preQ_0$ binding ($n_{H^+} \approx 0$). Interestingly, the D197H variant recovered proton uptake to a level almost analogous to that seen with the wildtype enzyme. The two variants of Cys190 showed reduced proton uptake as compared to the wildtype enzyme. In the H229A variant, the $preQ_0$ binding involved proton uptake larger than that in the wildtype enzyme.

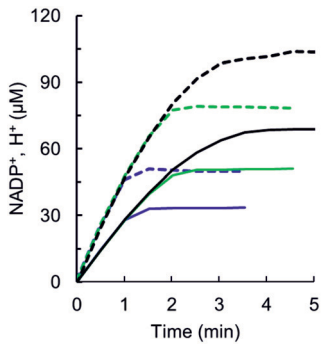

Fig. 5 Proton uptake (dashed lines) and $NADP^+$ formation (solid lines) during $preQ_0$ reduction by wildtype ecQueF are shown. Reaction conditions: 3.6 μM enzyme; 100 μM NADPH; 20, 30 and 40 μM $preQ_0$ (bottom to top, purple, green, and black). A Tris buffer (0.5 mM, pH 7.51) additionally containing 150 mM KCl and 34 μM phenol red was used.

Enzymatic reduction of $preQ_0$

Conversion of $preQ_0$ into $preQ_1$ was measured directly using HPLC.[17,27] As shown recently for certain ecQueF variants, 7-formyl-7-deazaguanine is released during a $preQ_0$ reduction

wherein the imine intermediate can hydrolyse due to its incomplete sequestration from the solvent in the enzyme (Scheme 1B).[27] Therefore, reactions were also analysed for 7-formyl-7-deazaguanine.

Under assay conditions routinely used with the wildtype enzyme[17] that involve measurement of NADPH consumption by absorbance at 340 nm, only the H229A variant showed activity. The k_{cat} of the variant was 0.30 (± 0.06) min^{-1}, that is, 24-fold lower than the k_{cat} of the wildtype enzyme (7.2 ± 0.1 min^{-1}).[17] Initial rates of the H229A variant showed saturation at low concentrations (≤ 1 μM) of both $preQ_0$ and NADPH. Determination of K_m was therefore not pursued. Using 4*R*-D-NADPH as a coenzyme, the kinetic isotope effect of 2.2 (± 0.2) on the k_{cat} of the H229A variant was determined. This is similar to the kinetic isotope effect of 2.4 on the k_{cat} of the wildtype enzyme.[17] When incubated for longer times (96 h) at high enzyme concentration (50 μM), a low level of nitrile reductase activity was confirmed for ecQueF Cys190 and Asp197 variants.

The loss of activity compared to the wildtype enzyme was substantial, about 10^4-fold for the Cys190 variants (C190A: 0.21×10^{-3} min^{-1}; C190S: 0.25×10^{-3} min^{-1}) and 10^5-fold for the Asp197 variants (D197A: 0.04×10^{-3} min^{-1}; D197H: 0.10×10^{-3} min^{-1}). Residual activity in these variants is interesting for it implies a reduction of the nitrile group that proceeds in the absence of a covalent ecQueF–$preQ_0$ intermediate. Careful control was therefore necessary to ascertain this activity beyond doubt.

First of all, a close balance between $preQ_0$ consumption and $preQ_1$ formation was demonstrated in all the reactions. 7-Formyl-7-deazaguanine was not released. Non-enzymatic conversion of $preQ_0$ by NADPH was not detected, indicating that catalysis from the ecQueF variants was required for the reaction.

Secondly, to ensure that the activity could not arise from an endogenous QueF contaminating the recombinant enzyme preparations used, we applied the *E. coli* cell extract to $preQ_0$ conversion. One cell extract was from the expression of the D197A variant, which was the least active among the enzymes analysed here. The other was from an *E. coli* strain harbouring the empty plasmid vector and treated identically as the positive control. Whereas the cell-extract containing D197A variant showed $preQ_1$ formation, the negative control was completely inactive. We also considered that proteins were purified by affinity *via* the His tag, and that the His tag was present in the recombinant but absent in the native enzyme.

Therefore, upon applying a purification procedure selective for the His-tagged target protein, it was inconceivable that a contaminating activity not detectable in the cell extract could become enriched to above detection limit in the course of purification.

Finally, interference from translational error, resulting in amino acid mis-incorporation to yield an active enzyme species, was unlikely due to the particular triplet codon changes used for site-directed mutagenesis. All codon changes involved substitutions of the first or second codon base (C190S, TGC → AGC; C190A, TGC → GCC; D197H, GAT → CAT, D197A, GAT → GCG; H229A, CAC → GCC). Translational misreading is however known to occur chiefly at the third base.[38–40] In summary, therefore, these results reinforced the suggestion that Cys190 and Asp197 variants of ecQueF retained a low level of nitrile reductase activity that was intrinsic to their respective active sites.

The pH dependence of $preQ_0$ reduction by the D197A variant was analysed by comparing reaction rates at pH 6.0, 7.5 and 9.0. The residual enzyme activity at pH 6.0 and pH 9.0, compared to the maximum activity at pH 7.5, was 19% and 24%, respectively. In a previous study,[24] the wildtype enzyme was shown to exhibit a similar pH dependence of activity in the pH range 6.0–9.0. Therefore, these results suggest that Asp197 is not responsible for the pH dependence of activity of ecQueF.

Catalytic proton transfer coupled to covalent catalysis in ecQueF

QueF crystal structures capture the elementary steps of $preQ_0$ binding.[18,21] Upon noncovalent complex formation, the

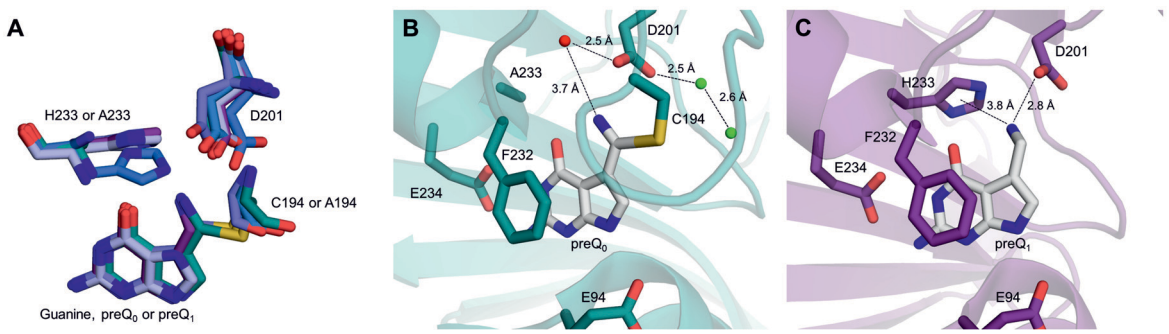

Fig. 6 Conformational flexibility of His and Asp residues in the vcQueF active site and binding of the $preQ_1$ product to the enzyme. (A) A structural overlay of vcQueF structures, used in Fig. 1 and 6, is shown: apo-enzyme (blue, C194A variant), holo-enzyme (deep blue, $preQ_0$–R262L variant; light blue, guanine–C194A variant; teal blue, $preQ_0$–H233A; violet, $preQ_1$–C194A variant) and ternary complex structures (purple blue, $preQ_0$–R262L variant–NADPH). (B) The covalent thioimidate complex of the vcQueF H233A variant with $preQ_0$ (PDB code: 4GHM, teal blue) is shown. The structure reveals that Asp201 interacts with water molecules both inside (red sphere) and outside (green sphere) the active site. This could establish a proton relay despite the absence of His. (C) The complex of vcQueF with $preQ_1$ (C194A variant, PDB code: 3RZP, violet) is shown. Crystal structures of vcQueF are from ref. 21 and from unpublished data in the database.

substrate is anchored tightly between the N-terminal ends of two helices (α2 and α5, in vcQueF; α1′ and α2, in bsQueF), as shown in Fig. 1D and E. The reactive nitrile group so becomes oriented towards the active-site loop comprising Cys190 and Asp197. The side chains of Asp197 and His229 adopt relatively flexible conformations that enable a dynamic, water-mediated interaction between the two residues (Fig. 6A). Upon covalent complex formation, the substrate nitrogen atom develops a hydrogen bond with Asp197, which in turn remains linked *via* a water molecule to His229 (Fig. 1A, B, and F). Biochemical evidence from the current study assigns proton relay function to this active-site network of hydrogen bonds.

The mechanism in Scheme 3 is proposed. Asp197 is central for proton transfer into and within the ecQueF active site. When $preQ_0$ binds, Asp197 picks up a proton from water to protonate His229. The relative proton amount taken up by the enzyme (~0.8 protons per active site) reflects the protonation state of the histidine at the pH of 7.5 used. Replacement of Asp197 by an alanine, whose side chain is incompetent in the proton transfer function considered, disrupts completely the proton uptake in conjunction with $preQ_0$ binding. Replacement by a histidine, by contrast, restores the proton uptake to a level (~0.6 protons per active site) comparable to that of the wildtype enzyme. The extra positive charge developed on the protonated His229 might assist in catalysis to covalent thioimidate formation. It could do so by promoting charge separation in the reactive nitrile group. Nucleophilic attack on carbon and proton transfer to nitrogen would thus be facilitated. Proton uptake by the H229A variant during $preQ_0$ binding was larger than it was in the wildtype enzyme. This probably reflects the protonation of a water molecule in the H229A active site (Scheme 4). Indeed, the covalent complex structure of the His233A variant of *Vibrio cholerae* QueF reveals a candidate water molecule hydrogen-bonded to the active-site aspartate (Fig. 6B).[21] Interestingly, as demonstrated by proton uptake measurements for the C190A and C190S variants of ecQueF, the catalytic cysteine is not essential for proton uptake during $preQ_0$ binding.

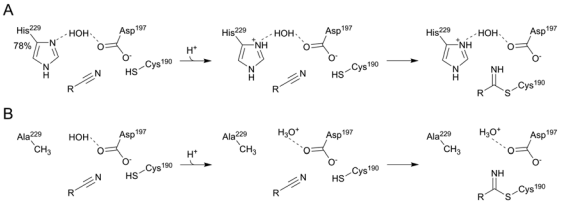

Scheme 4 Proton uptake upon covalent thioimidate formation in the ecQueF wildtype (A) and H229A variant (B) is shown at pH 7.5. The wildtype enzyme takes up about 0.78 protons due to the pK_a of His229 while the H229A variant takes up 1 proton by water. Amino acid numbering of ecQueF is used. The dashed line indicates hydrogen bonds.

The absolute requirement for Asp197 in covalent thioimidate formation is explained by a twofold role of this residue in catalytic proton transfer. First, Asp197 activates through deprotonation of Cys190 for function as the catalytic nucleophile. Second, Asp197 promotes the covalent thioimidate through catalytic proton transfer to the nitrile nitrogen atom. The nucleophilic attack on carbon probably occurs in concert with the Asp197-mediated proton transfer events, as shown in Scheme 3. Evidence in support of this notion is that the D197A and D197H variants were both completely inactive to form the covalent thioimidate even under conditions (pH ≥ 9.0) in which a cysteine would be expected to become (partially) deprotonated anyway.

As shown in Scheme 3, conversion of the covalent thioimidate to $preQ_1$ involves partial protonation–deprotonation, hence positive charge development, at the reactive nitrogen atom of the substrate. Proton relay *via* Asp197-water-His229 would help delocalizing the charge and could thus facilitate the hydride reduction from NADPH. Upon breakdown of covalent thiohemiaminal to noncovalently bound imine, Cys190 would become re-protonated *via* Asp197 in a reversion of the initializing proton transfer event. According to the mechanism proposed (Scheme 3), the $preQ_1$ product would feature an unprotonated amino group and proton uptake by $preQ_1$ probably takes place in solution. The notion is supported by

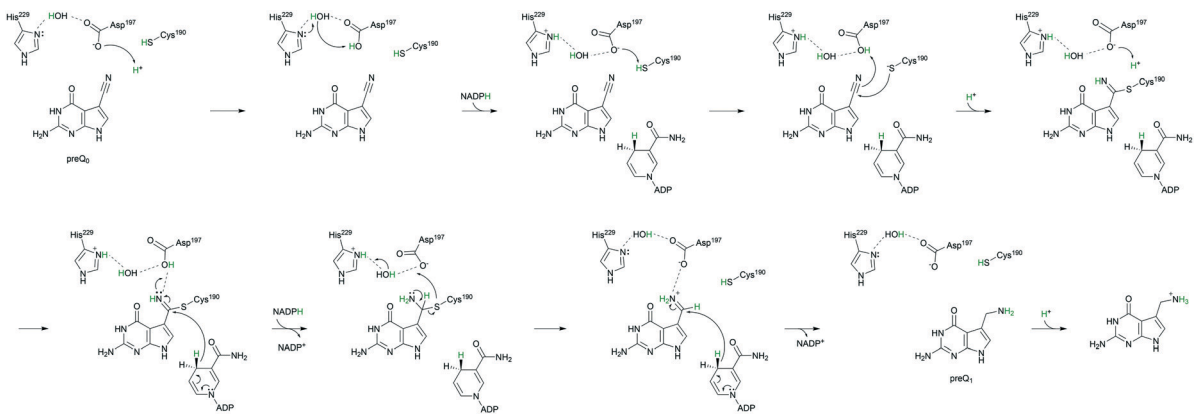

Scheme 3 Proposed enzymatic mechanism of reduction of $preQ_0$ to $preQ_1$ showing the proton transfers involved. Amino acid numbering of ecQueF is used. The dashed lines indicate hydrogen bonds. Protons and the NADPH hydride involved in the reaction are marked green.

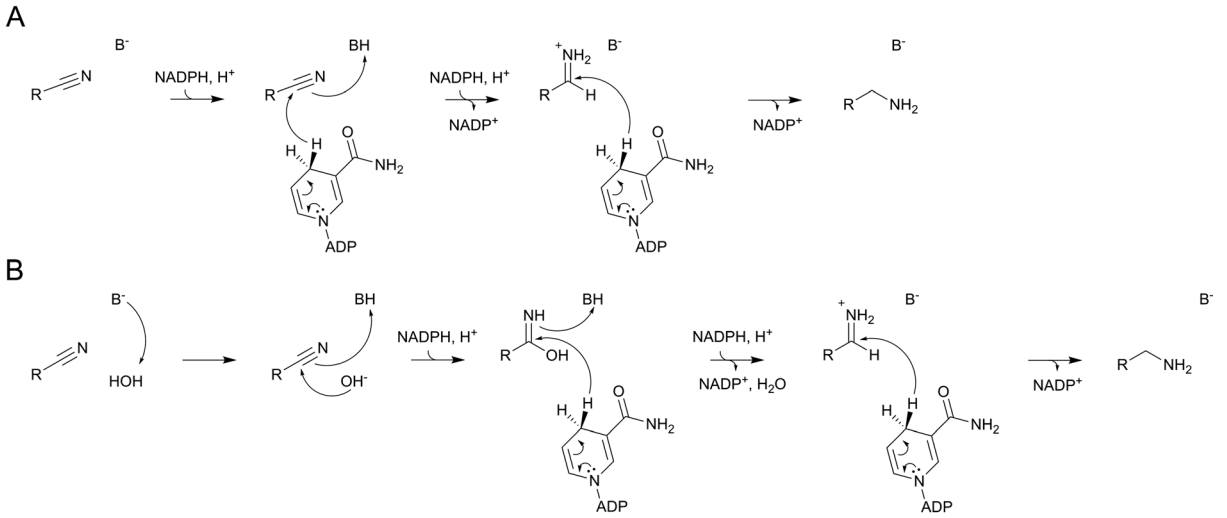

Scheme 5 Possible mechanisms of enzymatic nitrile reduction by NADPH in variants of ecQueF unable to form a covalent thioimidate enzyme intermediate. (A) Direct hydride reduction of nitrile. (B) Hydration nitrile followed by reduction. Both reactions may involve facilitation from an unassigned enzyme acid (BH) or base (B^-).

the structure of *V. cholerae* QueF in complex with $preQ_1$ (Fig. 6C). The structure shows the amino group of the product oriented towards the imidazole ring of His229. The orientation is suggestive of a cation–π interaction between the two groups, assuming the amino group to be protonated. The positioning of $preQ_1$ in the enzyme complex structure thus appears to be unproductive catalytically. Of note, the $preQ_1$ is not detectably oxidized by $NADP^+$ in the presence of ecQueF within a pH range (7.5–9.0) accessible to a stable enzyme.[17] The amino group pK_a of $preQ_1$ is predicted to be 8.39 (ChemSpider database). It may thus be difficult for the enzyme to bind $preQ_1$ in the presumably active, unprotonated form. From the evidence presented, an auxiliary role of His229 in each catalytic step of the QueF reaction is suggested (Scheme 3). This is consistent with the k_{cat} of the H229A variant being about 24-fold lower than the k_{cat} of the wildtype enzyme.

QueF and nitrilase appear to utilize a highly similar mechanism to promote the covalent thioimidate intermediate (Scheme 1A).[9,14,41] In the nitrilase, a triad of cysteine/glutamic acid/lysine constitutes the active-site apparatus.[8,16,41] Like Asp197 in QueF, the glutamic acid is central for catalytic nucleophile activation and for acid–base catalysis. The role adopted by the positively charged lysine in nitrilase might be similar to that proposed for the protonated His229 in QueF (Scheme 3).

Enzymatic nitrile reduction in the absence of covalent catalysis

The conversion of $preQ_0$ to $preQ_1$ by the C190A variant implies a nitrile reduction by NADPH that proceeds in the absence of a covalent enzyme intermediate. The Asp197 variants and the C190S variant both could form covalent intermediates with $preQ_0$ in principle, but no evidence in support of such intermediates was found in these enzymes. There is ample precedence for hydride reduction of nitriles to amines in synthetic organic chemistry.[42–44] Borane reagents are often used as hydride sources/donors.[43] The chemical conversions involve a twofold reduction at the nitrile carbon *via* the imine intermediate.[42,44] The catalytic reactions of the ecQueF variants might proceed analogously, using NADPH as the hydride donor (Scheme 5A). From its one-electron redox potential,[45–47] NADPH is able to reduce a nitrile group directly. An alternative possibility, shown in Scheme 5B, is that the reaction proceeds *via* base-catalysed attack of water on the nitrile group. Such conversion of the nitrile to iminol (amide) is well studied chemically.[48] The resulting iminol could then undergo two-fold reduction to the amine as shown. Note that our LC-MS analysis of the conversion of $preQ_0$ excludes the release of an amide (the iminol tautomer) or a carboxylic acid product in the enzymatic reactions. In both scenarios of Scheme 5, the enzyme might provide some catalytic facilitation from a general acid or base. Cys190 and Asp197 are candidates in the corresponding enzyme variants, but no clear assignment is possible on the evidence presented. Our results furthermore show that besides having the ability to position the nitrile substrate for the initial reaction (reduction or hydration–reduction; Scheme 5), the enzyme variants retain imine intermediate sequestration as a characteristic feature of the catalytic function of the ecQueF active site.[27] Therefore, each $preQ_0$ reduced by the variants, however slowly, makes it through to the $preQ_1$ product.

Conclusions

We show in this study that proton relay through an active-site network of hydrogen bonds is central for ecQueF to promote nitrile reduction to amine *via* a covalent thioimidate intermediate. Asp197 is the key residue to manage the interplay between

nucleophilic catalysis by Cys190 and the catalytic proton transfers. His229 has an auxiliary role. Deepened insight into the catalytic mechanism of ecQueF was thus obtained. The results have relevance in advancing mechanistic understanding of biological transformations of the nitrile group.

Conflicts of interest

There are no conflicts to declare.

Acknowledgements

This work has been supported by the Federal Ministry of Economy, Family and Youth (BMWFJ), the Federal Ministry for Transport, Innovation and Technology (BMVIT), the Styrian Business Promotion Agency SFG, the Vienna Business Agency, the Standortagentur Tirol, the Government of Lower Austria, and Styrian Provincial Government Economic Affairs and Innovation through the COMET-Funding Program managed by the Austrian Research Promotion Agency FFG. We thank Prof. Norbert Klempier and Dr. Birgit Wilding (Institute of Organic Chemistry, Graz University of Technology) for providing $preQ_0$, and Prof. Ruth Birner-Grünberger and B. Darnhofer (Diagnostic and Research Institute of Pathology & Omics Center Graz, Medical University of Graz) for protein-mass analysis.

References

1 A. J. M. Howden, C. Jill Harrison and G. M. Preston, *Plant J.*, 2009, **57**, 243–253.
2 A. J. M. Howden and G. M. Preston, *Microb. Biotechnol.*, 2009, **2**, 441–451.
3 V. M. Luque-Almagro, P. Cabello, L. P. Sáez, A. Olaya-Abril, C. Moreno-Vivián and M. D. Roldán, *Appl. Microbiol. Biotechnol.*, 2018, **102**, 1067–1074.
4 P. W. Ramteke, N. G. Maurice, B. Joseph and B. J. Wadher, *Biotechnol. Appl. Biochem.*, 2013, **60**, 459–481.
5 J.-S. Gong, J.-S. Shi, Z.-M. Lu, H. Li, Z.-M. Zhou and Z.-H. Xu, *Crit. Rev. Biotechnol.*, 2017, **37**, 69–81.
6 C. Brenner, *Curr. Opin. Struct. Biol.*, 2002, **12**, 775–782.
7 J.-S. Gong, Z.-M. Lu, H. Li, J.-S. Shi, Z.-M. Zhou and Z.-H. Xu, *Microb. Cell Fact.*, 2012, **11**, 142.
8 L. Zhang, B. Yin, C. Wang, S. Jiang, H. Wang, Y. A. Yuan and D. Wei, *J. Struct. Biol.*, 2014, **188**, 93–101.
9 S. Jiang, L. Zhang, Z. Yao, B. Gao, H. Wang, X. Mao and D. Wei, *Catal. Sci. Technol.*, 2017, **7**, 1122–1128.
10 B. Wilding, M. Winkler, B. Petschacher, R. Kratzer, A. Glieder and N. Klempier, *Adv. Synth. Catal.*, 2012, **354**, 2191–2198.
11 B. Wilding, M. Winkler, B. Petschacher, R. Kratzer, S. Egger, G. Steinkellner, A. Lyskowski, B. Nidetzky, K. Gruber and N. Klempier, *Chem. – Eur. J.*, 2013, **19**, 7007–7012.
12 S. G. Van Lanen, J. S. Reader, M. A. Swairjo, V. de Crécy-Lagard, B. Lee and D. Iwata-Reuyl, *Proc. Natl. Acad. Sci. U. S. A.*, 2005, **102**, 4264–4269.
13 L. Yang, S. L. Koh, P. W. Sutton and Z.-X. Liang, *Catal. Sci. Technol.*, 2014, **4**, 2871.
14 B. C. M. Fernandes, C. Mateo, C. Kiziak, A. Chmura, J. Wacker, F. van Rantwijk, A. Stolz and R. A. Sheldon, *Adv. Synth. Catal.*, 2006, **348**, 2597–2603.
15 H. C. Pace, S. C. Hodawadekar, A. Draganescu, J. Huang, P. Bieganowski, Y. Pekarsky, C. M. Croce and C. Brenner, *Curr. Biol.*, 2000, **10**, 907–917.
16 J. E. Raczynska, C. E. Vorgias, G. Antranikian and W. Rypniewski, *J. Struct. Biol.*, 2011, **173**, 294–302.
17 J. Jung, T. Czabany, B. Wilding, N. Klempier and B. Nidetzky, *J. Biol. Chem.*, 2016, **291**, 25411–25426.
18 V. M. Chikwana, B. Stec, B. W. K. Lee, V. de Crécy-Lagard, D. Iwata-Reuyl and M. A. Swairjo, *J. Biol. Chem.*, 2012, **287**, 30560–30570.
19 B. W. K. Lee, S. G. Van Lanen and D. Iwata-Reuyl, *Biochemistry*, 2007, **46**, 12844–12854.
20 L. Gjonaj, M. Pinkse, E. Fernández-Fueyo, F. Hollmann and U. Hanefeld, *Catal. Sci. Technol.*, 2016, **6**, 7391–7397.
21 Y. Kim, M. Zhou, S. Moy, J. Morales, M. A. Cunningham and A. Joachimiak, *J. Mol. Biol.*, 2010, **404**, 127–137.
22 D. Iwata-Reuyl, *Bioorg. Chem.*, 2003, **31**, 24–43.
23 P. Domínguez de María, *ChemCatChem*, 2011, **3**, 1683–1685.
24 K. Moeller, G.-S. Nguyen, F. Hollmann and U. Hanefeld, *Enzyme Microb. Technol.*, 2013, **52**, 129–133.
25 M. Li, Z. Zhou, Z.-J. Zhang, H.-L. Yu and J.-H. Xu, *J. Mol. Catal. B: Enzym.*, 2016, **131**, 47–54.
26 Z. Zhou, M. Li, J.-H. Xu and Z.-J. Zhang, *ChemBioChem*, 2018, **19**, 521–526.
27 J. Jung and B. Nidetzky, *J. Biol. Chem.*, 2018, **293**, 3720–3733.
28 A. J. M. Ribeiro, L. Yang, M. J. Ramos, P. A. Fernandes, Z.-X. Liang and H. Hirao, *ACS Catal.*, 2015, **5**, 3740–3751.
29 B. El Yacoubi, M. Bailly and V. de Crécy-Lagard, *Annu. Rev. Genet.*, 2012, **46**, 69–95.
30 F. Harada and S. Nishimura, *Biochemistry*, 1972, **11**, 301–308.
31 A. Mohammad, A. Bon Ramos, B. W. K. Lee, S. W. Cohen, M. Kiani, D. Iwata-Reuyl, B. Stec and M. Swairjo, *Biomolecules*, 2017, **7**, 30.
32 W. Wang and B. A. Malcolm, *BioTechniques*, 1999, **26**, 680–682.
33 A. G. Kozlov and T. M. Lohman, *Biochemistry*, 1999, **38**, 7388–7397.
34 S. Leavitt and E. Freire, *Curr. Opin. Struct. Biol.*, 2001, **11**, 560–566.
35 R. N. Goldberg, N. Kishore and R. M. Lennen, *J. Phys. Chem. Ref. Data*, 1999, **31**, 231–370.
36 S. L. Pival, M. Klimacek and B. Nidetzky, *Biochem. J.*, 2009, **421**, 43–49.
37 M. Klimacek, M. Brunsteiner and B. Nidetzky, *J. Biol. Chem.*, 2012, **287**, 6655–6667.
38 J. M. Ogle and V. Ramakrishnan, *Annu. Rev. Biochem.*, 2005, **74**, 129–177.
39 J. M. Ogle, D. E. Brodersen, W. M. Clemons Jr., M. J. Tarry, A. P. Carter and V. Ramakrishnan, *Science*, 2001, **292**, 897–902.
40 M. Johansson, J. Zhang and M. Ehrenberg, *Proc. Natl. Acad. Sci. U. S. A.*, 2012, **109**, 131–136.

41 L. Martínková and V. Křen, *Curr. Opin. Chem. Biol.*, 2010, **14**, 130–137.
42 D. B. Bagal and B. M. Bhanage, *Adv. Synth. Catal.*, 2015, **357**, 883–900.
43 D. Haddenham, L. Pasumansky, J. DeSoto, S. Eagon and B. Singaram, *J. Org. Chem.*, 2009, **74**, 1964–1970.
44 C. Bornschein, S. Werkmeister, B. Wendt, H. Jiao, E. Alberico, W. Baumann, H. Junge, K. Junge and M. Beller, *Nat. Commun.*, 2014, **5**, 4111.
45 K. Burton and T. H. Wilson, *Biochem. J.*, 1953, **54**, 86–94.
46 A. W. Munro, M. A. Noble, L. Robledo, S. N. Daff and S. K. Chapman, *Biochemistry*, 2001, **40**, 1956–1963.
47 T. E. DeCoursey, D. Morgan and V. V. Cherny, *Nature*, 2003, **422**, 531–534.
48 T. E. Schmid, A. Gómez-Herrera, O. Songis, D. Sneddon, A. Révolte, F. Nahra and C. S. J. Cazin, *Catal. Sci. Technol.*, 2015, **5**, 2865–2868.